



# MHD Stagnation-Point Flow and Heat Transfer in a Micropolar Fluid over an Exponentially Vertical Sheet

Fairul Naim Abu Bakar<sup>1</sup>, Siti Khuzaimah Soid<sup>1,\*</sup>

<sup>1</sup> Faculty of Computer and Mathematical Sciences, Universiti Teknologi MARA, 40450 Shah Alam, Selangor, Malaysia

## ARTICLE INFO

### Article history:

Received 29 May 2022

Received in revised form 15 June 2022

Accepted 20 July 2022

Available online 1 March 2023

### Keywords:

Micropolar fluid; MHD; stagnation point flow; heat transfer; exponentially stretching/shrinking sheet; mixed convection

## ABSTRACT

This paper examines the magneto hydrodynamic (MHD), stagnation-point flow and heat transfer caused by an exponentially stretching/shrinking vertical sheet and the presence of mixed convection (buoyancy effect) in a micropolar fluid. A set of variables is employed to transform the system of partial differential equations (PDEs) to ordinary differential equations (ODEs). The ODEs are then numerically solved in MATLAB software using BVP4c. There are a lot of agreements when compared to previous findings. The impacts of different parameters, such as micropolar, magnetic, mixed convection, radiation, temperature, and stretching/shrinking parameters are displayed graphically. It is found that contradictory phenomena between Micropolar and mixed convection for fluid velocity, angular velocity and temperature distribution profiles. The velocity profile at the vertical plate increases due to the increasing buoyancy, magnetic and radiation parameters. The particle rotation occurs in two phenomena for buoyancy and magnetic parameters and it is reversible for micropolar. The temperature of the fluid decreases with buoyancy and magnetic parameters.

## 1. Introduction

The study of the flow over-stretching and shrinking attracts attention among researchers. Various applications in the shrinking film, capillary effects in small pores, the shrinking-swell behavior, hydraulic properties of agricultural clay soils, and a rising shrinking balloon are important to industries and the engineering field [1]. While stretching surface has various uses in many manufacturing processes, such as the extrusion of molten polymers owing to the slit die in the creation of plastic sheets, paper production, wires, and the fiber coating process of foodstuffs. Furthermore, the stagnation point flow with heat transfer across a stretching and shrinking sheet has several industrial uses. Some applications include boundary layer along material handling conveyors, blood flow difficulties, aerodynamics, plastic sheet extrusion, cooling of metallic plates in a bath, textile and paper industries, and so forth [2]. According to Crane [3], Hiemenz was the first to investigate it, demonstrating that using similarity transformation, the Navier-Stokes equations regulating the flow can be reduced to an ordinary differential equation of third order. Because of the

\* Corresponding author.

E-mail address: [khuzaimah@tmsk.uitm.edu.my](mailto:khuzaimah@tmsk.uitm.edu.my) (Siti Khuzaimah Soid)

nonlinearities in the reduced differential equation, no analytical solution is accessible, and the nonlinear equation is normally solved numerically with two-point boundary conditions, one of which is set to infinity.

Micropolar fluid, which includes liquid crystals, polymeric suspensions, and animal blood, is an example of a non-Newtonian fluid. Micropolar fluid flow research arose from studies of biological molecular machinery, atherogenesis, microcirculation, and microfluidics. The concept is based on spinning particles, the rotation of which is defined by an independent microrotation vector [4]. These fluids resemble rigid molecules, magnetic fluids, dusty clouds, muddy fluids, and biological fluids [5]. The problem of stagnation point flow in a micropolar fluid has been extended in numerous ways to include various physical effects [6-15].

Many academics have examined the non-uniqueness of solutions to fluid flow issues on moving, shrinking, and stretching sheets in the presence and absence of a buoyancy effect in the last few years [16-24].

The research was focused on the magnetic characteristics of electrically conducting fluids and was called MHD (Magnetohydrodynamic). The study of magnetic properties and behavior of electrically conducting fluids is known as MHD. It is made up of liquid and magnetic properties, adjoined particles are affected by magnetic fields and their concentration in the fluid regime has been rearranged. Geothermal energy extraction, plastic sheets, nuclear reactor cooling, blood flow difficulties, plasma research, subsurface electric cable cooling, and artificial fibers are all examples of these applications [25]. The study on MHD has been extended in numerous ways [26-29].

Motivated by earlier study from Soid *et al.*, [4], the present work intends to explore the MHD stagnation point flow and heat transfer over an exponentially stretching/shrinking vertical sheet submerged in a micropolar fluid with a buoyancy effect. In this research, we added buoyancy parameter, heat transfer and exponential on similarity variables. Our objectives are to design the mathematical models of micropolar fluid with buoyancy effect, construct the mathematical formulation, design algorithms and interpret graphically. On other hand, it is to analyze the effect on velocity, angular velocity and temperature profiles. Similarity variables were employed to turn the governing partial differential equations (PDEs) into ordinary differential equations (ODEs). The amended equations were then numerically solved in MATLAB using BVP4c. We expect that the results gained will be beneficial for applications and as a supplement to prior research.

## 2. Methodology

Consider a micropolar fluid flow towards a stagnation point on a vertical sheet as illustrated in Figure 1. The designed was exactly based on the original profile of Waini *et al.*, [30] that studied about hybrid nanofluid flow towards a stagnation point on an exponentially stretching/shrinking vertical sheet with buoyancy effects. Therefore, this present work is dealing with micropolar fluid by extend the work by Soid *et al.*, [4]. Figure 1 depicts a model for several real-world applications such as electronic cooling and cooling of a metallic plate. This research could help the industry create more efficient gadgets related to the heat transfer process. The  $x$  and  $y$  axes are Cartesian coordinates where  $x$  is assigned vertically along the surface and  $y$  is orthogonal to it with the origin  $o$ . The symbol  $u_e(x) = ae^{x/L}$  is free stream velocity where  $a > 0$  (constant) and  $L$  is reference length. Next,  $u_w(x) = be^{x/L}$  is an exponential velocity when the surface is stretched ( $b > 0$ ), shrunk ( $b < 0$ ) or  $b = 0$  is for the static surface. The surface temperature is given as  $T_w(x) = T_\infty + T_0 e^{2x/L}$  where  $T_0$  is a constant and  $T_\infty$  is the ambient temperature. Hence,  $g$  is a symbol of acceleration due to gravity.

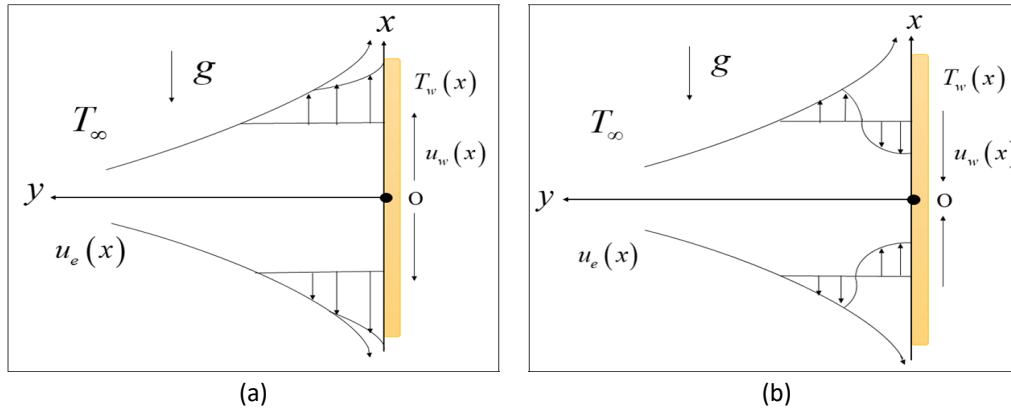


**Fig. 1.** The geometry of the flow problem of (a) Stretching and (b) Shrinking sheet

The current work is solely concerned with the buoyancy effects in a mixed convection flow of micropolar fluid approaching a stagnation point on an exponentially stretching/shrinking vertical sheet. It also shows the solutions for a single parameter value for stretching and shrinking, as well as buoyancy assisting and opposing flow. The governing boundary layer parabolic partial differential equations (PDEs) are written as continuity, linear momentum, angular momentum and energy equations [1,30,31]:

$$\frac{\partial u}{\partial x} + \frac{\partial v}{\partial y} = 0 \quad (1)$$

$$u \frac{\partial u}{\partial x} + v \frac{\partial u}{\partial y} = u_e \frac{\partial u_e}{\partial x} + \left( \nu + \frac{\kappa}{\rho} \right) \frac{\partial^2 u}{\partial y^2} + \frac{\kappa}{\rho} \frac{\partial N}{\partial y} + g \beta_T (T - T_\infty) - \frac{\sigma B^2}{\rho(u - u_e)} \quad (2)$$

$$u \frac{\partial N}{\partial x} + v \frac{\partial N}{\partial y} = \frac{\chi}{\rho j} \frac{\partial^2 N}{\partial y^2} - \frac{\kappa}{\rho j} \left( 2N + \frac{\partial u}{\partial y} \right) \quad (3)$$

$$u \frac{\partial T}{\partial x} + v \frac{\partial T}{\partial y} = \frac{k}{\rho c_p} \frac{\partial^2 T}{\partial y^2} - \frac{1}{\rho c_p} \frac{\partial q_r}{\partial y} \quad (4)$$

The boundary requirements must be satisfied at all points along the boundary of a region in order for a set of differential conditions to be solved. The boundary conditions applicable to the flow are:

$$\begin{aligned} u = u_w, v = 0, T = T_w, N = -m \frac{\partial u}{\partial y} \text{ at } y = 0 \\ u \rightarrow u_e, T \rightarrow T_\infty, N \rightarrow 0 \text{ as } y \rightarrow \infty \end{aligned} \quad (5)$$

where  $u$  and  $v$  are component of velocity along  $x$  and  $y$  direction respectively. The symbol  $\nu = \mu / \rho$  is the kinematic viscosity,  $\rho$  is the fluid density,  $\mu$  is the coefficient of fluid viscosity,  $N$  is microrotation or angular velocity,  $j = 2L\nu e^{-x/L} / a$  is micro-inertia per unit mass,  $\chi = \mu(1 + K/2)j$  is spin gradient,  $\kappa$  is the vortex viscosity. The electrical conductivity of the fluid

assigned as  $\sigma$ ,  $B(x) = B_0 e^{x/2L}$  is the variable magnetic field where  $B_0$  is a constant and  $c_p$  is the specific heat. The symbol  $\beta_T$  is the thermal expansion coefficient. Eq. (1) to Eq. (4) along with the boundary condition Eq. (5) can be expressed in a simpler form by introducing the following similarity transformation [30]:

$$\eta = \sqrt{\frac{a}{2\nu L}} e^{\frac{x}{2L}} y, \quad u = a e^{\frac{x}{2L}} f'(\eta), \quad v = -\sqrt{\frac{a\nu}{2L}} e^{\frac{x}{2L}} (f(\eta) + \eta f'(\eta)), \quad \theta(\eta) = \frac{T - T_\infty}{T_w - T_\infty},$$

$$N = a \sqrt{\frac{a}{2\nu L}} e^{\frac{3x}{2L}} h(\eta) \tag{6}$$

Where  $\eta$  is similarity variable, while  $u$  and  $v$  denotes the stream function that the continuity Eq. (1) is identically fulfilled. Thus, the transformed linear momentum Eq. (2), angular momentum Eq. (3) and energy Eq. (4) become:

$$f'''(1 + K) + f''f - 2(f')^2 - M(f' - 1) + K h' + 2\lambda\theta + 2 = 0$$

$$(1 + K/2)h'' - K(2h + f'') - 3f'h + f h' = 0 \tag{7}$$

$$\text{Pr}(4f'\theta - f\theta') - \theta''(1 + 4R/3) = 0$$

The corresponding boundary conditions:

$$f(\eta) = 0, f'(\eta) = \varepsilon, \theta(\eta) = 1, h(\eta) = -mf''(\eta) \text{ at } \eta = 0$$

$$f'(\eta) \rightarrow 1, \theta(\eta) \rightarrow 0, h(\eta) \rightarrow 0 \text{ as } \eta \rightarrow \infty \tag{8}$$

where the prime indicates differentiation with respect to  $\eta$  and  $M = 2\sigma B_0^2 L / \rho a$  is Hartmann number or magnetic parameter.  $\lambda = g\beta_T T_0 L / a^2$  is buoyancy parameter,  $\varepsilon = b/a$  is the stretching/shrinking parameter where  $a > 0$  (constant) and the surface is stretched ( $b > 0$ ) or shrunk ( $b < 0$ ). Therefore, the value of  $\varepsilon$  is directly proportional to  $b$ . Next,  $K = \kappa / \mu$ ,  $\text{Pr} = \mu c_p / k$  and  $R = 4\sigma^* T_\infty^3 / k^*$  are the micropolar parameter, Prandtl number and the radiation parameter respectively. These transformed equations are comparable to the previous studied such as the study of Hybrid nanofluid flow towards a stagnation point on an exponentially stretching/shrinking vertical sheet with buoyancy effects by Waini *et al.*, [30]. Next was Uddin *et al.*, [31], the study of micropolar fluid flow and heat transfer over an exponentially permeable shrinking sheet. Finally, from Siddiqua *et al.*, [32], the effect of thermal radiation on conjugate natural convection flow of a micropolar fluid along a vertical surface.

The involved physical quantities are the skin friction coefficient  $C_f$ , the local Nusselt number  $Nu_x$  and the local couple stress  $M_x$  [10]:

$$C_f = \frac{\tau_w}{\rho u_e^2}, M_x = \frac{\chi \left( \frac{\partial N}{\partial y} \right)_{y=0}}{\rho x u_e^2}, Nu_x = -\frac{x}{(T_w - T_\infty)} \frac{\partial T}{\partial y}_{y=0} \quad (9)$$

Where the surface shear stress  $\tau_w = \left[ (\mu + \kappa) \partial u / \partial y + \kappa N \right]_{y=0}$ . Then, the reduced skin friction coefficient, the local couple stress, and the reduced local Nusselt number:

$$C_f (Re_x)^{1/2} \sqrt{\frac{2L}{x}} = \left[ 1 + (1-m)K \right] f''(0), M_x Re_x = \left( 1 + \frac{K}{2} \right) h'(0)$$

$$Nu_x (Re_x)^{1/2} \sqrt{\frac{2L}{x}} = -\theta'(0) \quad (10)$$

$Re_x = x u_e / \nu$  is the local Reynolds number.

### 3. Results and Discussion

An analysis of the behaviors of the velocity, angular, and temperature profiles is carried out. The numerical solutions are obtained using BVP4c in MATLAB. The numerical values of  $C_f (Re_x)^{1/2} \sqrt{2L/x}$  and  $Nu_x (Re_x)^{1/2} \sqrt{2L/x}$  are obtained for various values of stretching/shrinking parameter  $\varepsilon$ , when  $Pr = 6.2$  and non-buoyant case  $\lambda = 0$  with other parameter was set to be constant at  $K = M = m = R = 0$ . Table 1 and Table 2 show the comparison of the skin friction coefficient and the local Nusselt number between the results found by Waini *et al.*, [30] and Rehman *et al.*, [33] with the present study, respectively.

The current results were in great agreement with the earlier study when the numbers in Table 1 and Table 2 were compared. As a result, the approach employed for this study was valid and accurate to verified. The values of the skin friction coefficient decrease while the values of the local Nusselt number increase when the parameter stretches/shrinking increases.

**Table 1**

Comparison for Numerical Values  $C_f (Re_x)^{1/2} \sqrt{2L/x}$  for  $\varepsilon = -0.5, 0, 0.5$

$\varepsilon$	Waini <i>et al.</i> , [30]	Rehman <i>et al.</i> , [33]	Present Study
-0.5	2.1182		2.11816867
0	1.6872	1.68720	1.68721817
0.5	0.9604	0.96040	0.96041608

**Table 2**

Comparison for Numerical Values  $Nu_x (Re_x)^{1/2} \sqrt{2L/x}$  for  $\varepsilon = -0.5, 0, 0.5$

$\varepsilon$	Waini <i>et al.</i> , [30]	Present Study
-0.5	0.0588	0.05878644
0	2.5066	2.50662545
0.5	4.8016	4.08157327

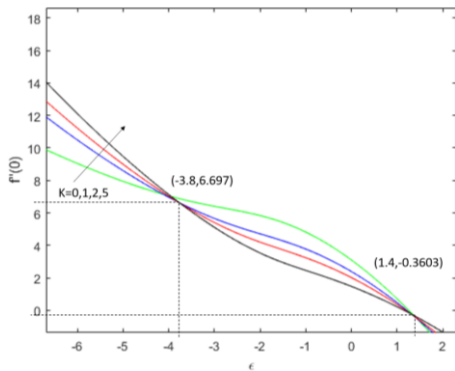
Parameters of micropolar  $K$ , buoyancy  $\lambda$ , magnetic  $M$  and radiation  $R$  will be examine. The other parameters such as material parameter  $m$  and Prandtl number  $Pr$  are fixed to  $m=0.5$  and  $Pr=6.2$  are considered. The physical parameters have been selected regarding the previous research such as Prandtl number from Waini *et al.*, [30], Stretching/shrinking and material parameter from Soid *et al.*, [4], and the others are from Song *et al.*, [17], Reddy *et al.*, [34], Mutegi *et al.*, [35], and Abdul Halim and Mohd Noor [36].

Figure 2 illustrates that when the micropolar parameter increases, so does the skin friction coefficient. As a result, the fluid’s mobility on the surface become tough at  $\varepsilon < -4$ . The fluid become smooth at  $\varepsilon \approx -3.8$ . When  $\varepsilon \approx 1.4$  the fluid moves are changing as previously but more smoothly and it show the drag force is approximate to zero (no drag force). From previous paper, the skin friction decreases due to increment of micropolar parameter. This is may be because of the present of buoyancy parameter.

Figure 3 shows an increase in the value of the micropolar parameter led to an increase of the local couple stress. The couple stress is related to a particle rotational speed gradient on the surface. It also shows the local couple stress become decreases when  $-1.5 < \varepsilon < 1.3$  and increases again due to the stretch. This phenomenon is reversible to the research by Soid *et al.*, [4] where the couple stress decreases for shrinking and increases for stretching.

When the values of the surface shear stress and the local couple stress are zero, there is a noticeable sign, especially when the plate and fluid velocity are approximate equal at  $\varepsilon = 1$ . In terms of physics, zero surface shear stress occurs when the fluid and solid surfaces move at the same speed, resulting in no friction at the fluid-solid interface. While, the couple stress is zero, it may be due to the non-effect of micro-structure, which causes the particle at the surface to be unable to rotate in a zero-gradient rotation.

The local Nusselt number decreases as the micropolar parameter rises as shown in Figure 4. This is may be due to heat exchange from the surface through the fluid for shrinking ( $\varepsilon < 0$ ). For the stretching ( $\varepsilon > 0$ ), there is no heat exchange due to the value of the local Nusselt number is approximately equal to zero. This is because of the temperature of the fluid and the surface are equal.



**Fig. 2.** Skin friction coefficient  $f''(0)$  for varies of  $K$

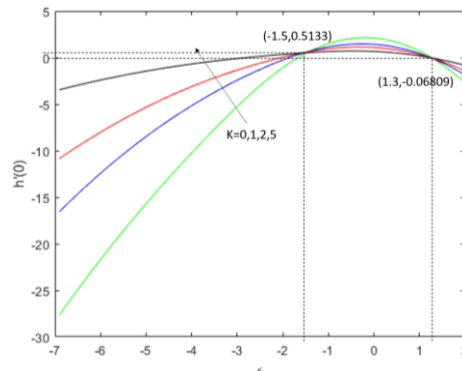


**Fig. 3.** Couple stress  $h'(0)$  for varies of  $K$

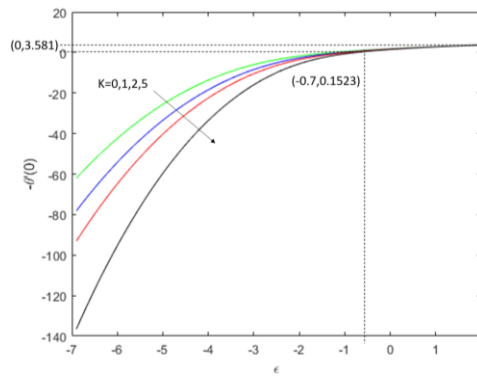


**Fig. 4.** Nusselt number  $-\theta'(0)$  for varies of  $K$

The Figure 5, Figure 6 and Figure 7 demonstrate the impacts of skin friction coefficient  $f''(0)$ , the local couple stress  $h'(0)$ , and the local Nusselt number  $-\theta'(0)$  on the values of magnetic parameter  $M$  respectively. The parameters' values are  $M=0,0.5,1,2$ ,  $m=0.5$ ,  $Pr=6.2$  and  $\lambda=K=R=2$ .

As the magnetic field increases, the solution become wider in all figure. The skin friction coefficient exhibits two phenomena which are it grows to  $\epsilon \approx 0.9$  and reduces to stretch surface roughly  $\epsilon > 0.9$ , as seen in Figure 5. In Figure 6, the local couple stress is reduces to  $\epsilon \approx -5.5$ , then increased to  $\epsilon \approx 0.9$ , and then decreased again to stretch surface approximately  $\epsilon > 0.9$ . Figure 7 depicts the rise in the local Nusselt number due to the increment for magnetic parameter. It also indicates that at the stretching surface ( $\epsilon > 0$ ), the local Nusselt number converge to  $-\theta'(0) \approx 2.27$ . The presence of magnetic field imposes viscous drag forces on the flow field, causing the fluid's velocity to decelerate and thereby increasing the skin coefficient on the surface. This is due to the Lorentz force, which provides a resistive force against the flow, causing the fluid's velocity to slow.

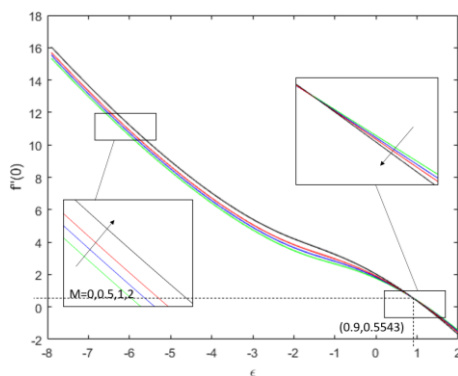


**Fig. 5.** Skin friction coefficient  $f''(0)$  for varies of  $M$

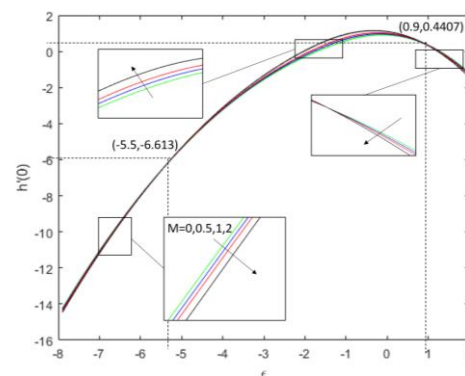


**Fig. 6.** Couple stress  $h'(0)$  for varies of  $M$

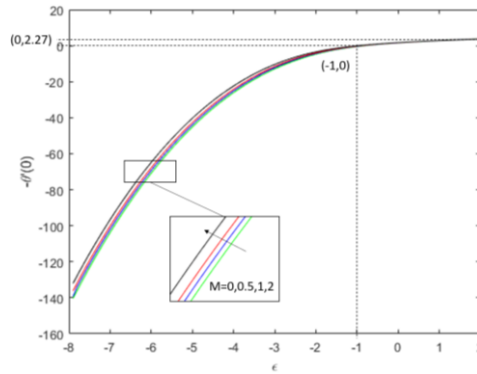


**Fig. 7.** Nusselt number  $-\theta'(0)$  for varies of  $M$

The Figure 8, Figure 9 and Figure 10 below show the effects of Skin friction coefficient  $f''(0)$ , the local couple stress  $h'(0)$ , and the local Nusselt number  $-\theta'(0)$  on the buoyancy parameter  $\lambda$  values, respectively. The values of the parameters are  $\lambda=0,1,2,3$ ,  $m=0.5$ ,  $Pr=6.2$  and  $M=K=R=2$ .

The increase in the buoyancy parameter raises the values of the skin friction coefficient in Figure 8, the local couple stress in Figure 9 and also the local Nusselt number in Figure 10. We can observe that when there is no buoyancy effect ( $\lambda=0$ ), the outcome in a shrinking plate ( $\epsilon < 0$ ) becomes wider same as the previous finding. Figure 8 depicts how the drag force reduces when stretching plate ( $\epsilon > 0$ ). Meanwhile, Figure 9 shows the upper and lower trends for the particle rotation when shrinking and stretching plates. Figure 9 illustrates how heat is transferred from the fluid to the vertical plate as it stretches.

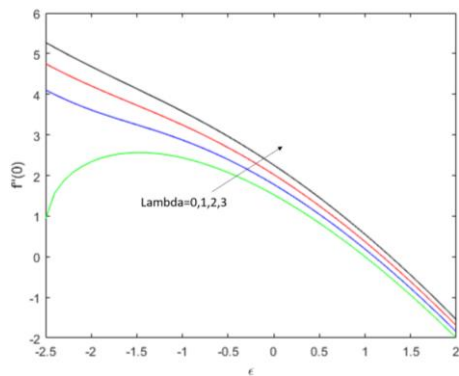


**Fig. 8.** Skin friction coefficient  $f''(0)$  for varies of  $\lambda$

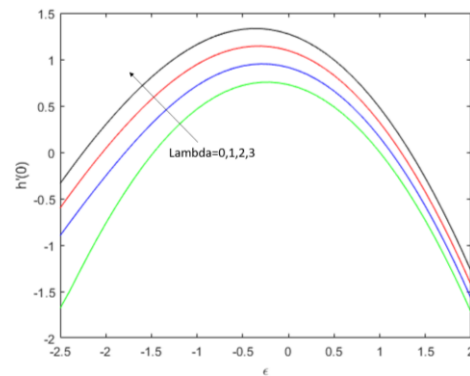


**Fig. 9.** Couple stress  $h'(0)$  for varies of  $\lambda$



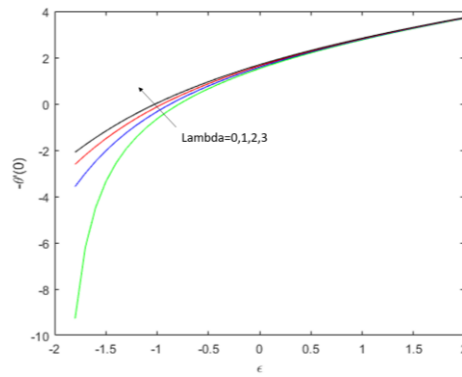


**Fig. 10.** Nusselt number  $-\theta'(0)$  for varies of  $\lambda$

The Figure 11, Figure 12 and Figure 13 below show the effects of Skin friction coefficient  $f''(0)$ , the local couple stress  $h'(0)$ , and the local Nusselt number  $-\theta'(0)$  on the values of radiation parameter  $R$ , respectively. The values for each parameter are  $R=0,1,3,5$ ,  $m=0.5$ ,  $Pr=6.2$  and  $M=K=\lambda=2$ .

Figure 11 shows that when the radiation parameter rises, the skin friction coefficient drops to  $\epsilon \approx -1$  and the drag force for stretching plate ( $\epsilon > 0$ ) increases with relatively low values ( $f''(0) < 3.3$ ). Figure 12 shows that the local couple stress falls to  $\epsilon \approx -1$  and increases when the plate is stretched. In Figure 13, the local Nusselt number rises to  $\epsilon \approx -0.4$  and falls for stretched plate.

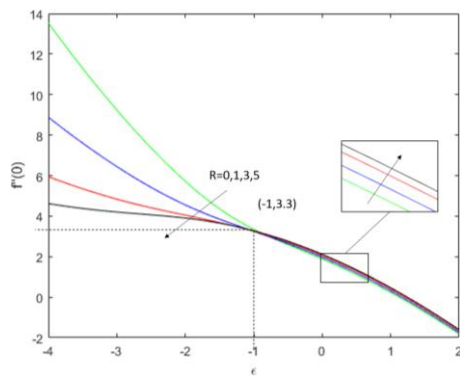


**Fig. 11.** Skin friction coefficient  $f''(0)$  for varies of  $R$

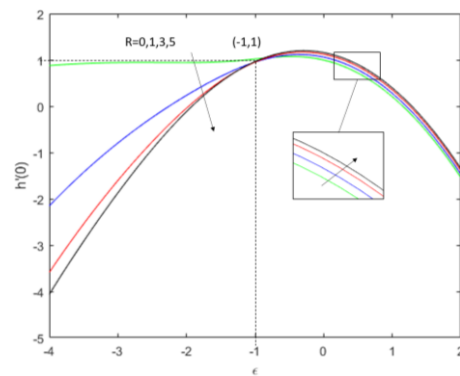


**Fig. 12.** Couple stress  $h'(0)$  for varies of  $R$

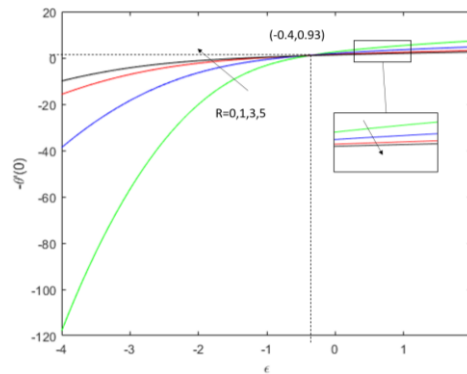


**Fig. 13.** Nusselt number  $-\theta'(0)$  for varies of  $R$

The effects on the velocity  $f'(\eta)$ , the angular velocity  $h(\eta)$ , and the temperature  $\theta(\eta)$  profiles are graphically presented. This result is focusing for shrinking plate where the ratio is 1 ( $\epsilon = -1$ ).

The Figure 14, Figure 15 and Figure 16 illustrate the effects of the velocity  $f'(\eta)$ , the angular velocity  $h(\eta)$ , and the temperature  $\theta(\eta)$  profiles on the values of micropolar parameter  $K$  respectively. The values for physical parameters are  $K = 0, 1, 2, 5$  and  $\lambda = M = R = 2$ . These profiles asymptotically satisfy the boundary condition in Eq. (8), giving us confidence in the solutions' accuracy. The decreasing behavior of  $f'(\eta)$  is observed with the increase of  $K$  as shown in Figure 14. The behavior of  $h(\eta)$  is given in Figure 15. It is illustrated that  $h(\eta)$  increases to  $h(\eta) \approx -0.5$  and decreases to the boundary condition with increasing of  $K$ . The current results from velocity and angular profiles show the same behavior to the previous finding. Meanwhile, Figure 16 shows  $\theta(\eta)$  increases due to increasing of  $K$ .

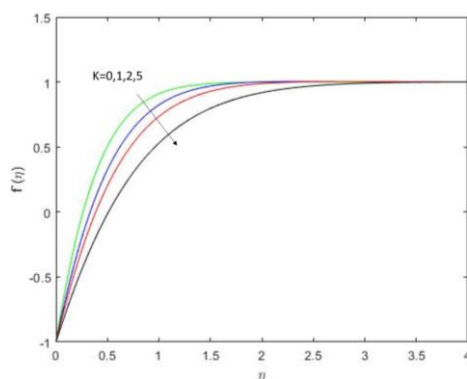


**Fig. 14.** Velocity profile  $f'(\eta)$  for varies of  $K$

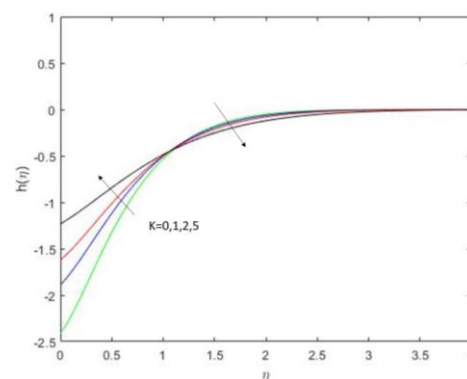


**Fig. 15.** Angular velocity profile  $h(\eta)$  for varies of  $K$

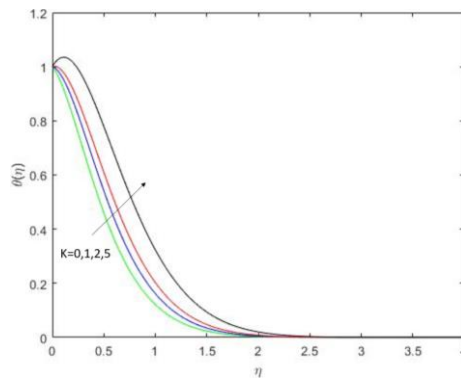


**Fig. 16.** Temperature profile  $\theta(\eta)$  for varies of  $K$

The Figure 17, Figure 18 and Figure 19 show the effects on magnetic parameter  $M$  where  $M = 0, 0.5, 1, 2$ . These phenomena are opposite to the effect on micropolar parameter which are the velocity, the angular velocity and temperature profiles. As shown in the Figure 17, the fluid velocity increases also wider the graph. The behavior of  $h(\eta)$  shows the  $M$  decreases to the  $h(\eta) \approx -0.4$  and increase to boundary condition. The  $\theta(\eta)$  decreases due to the present of  $M$ .

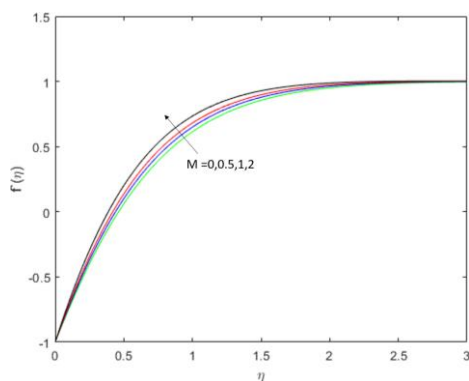


**Fig. 17.** Velocity profile  $f'(\eta)$  for varies of  $M$

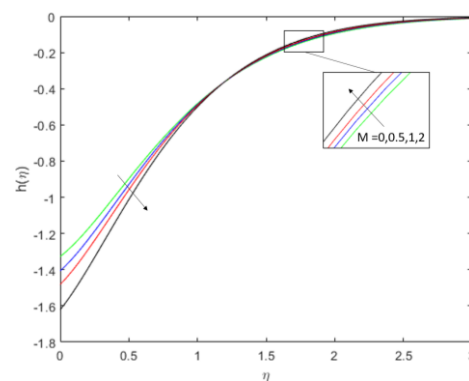


**Fig. 18.** Angular velocity profile  $h(\eta)$  for varies of  $M$

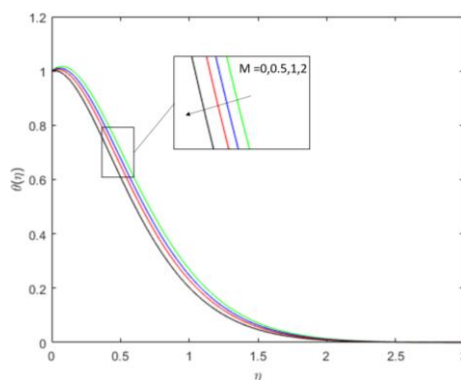


**Fig. 19.** Temperature profile  $\theta(\eta)$  for varies of  $M$

The Figure 20, Figure 21 and Figure 22 show the effects of  $f'(\eta)$ ,  $h(\eta)$ , and  $\theta(\eta)$  on the buoyancy parameter  $\lambda$  values, respectively. There is an opposite phenomenon with micropolar effect. The value of the buoyancy parameters is  $\lambda=0,1,2,3$  and micropolar parameter  $K=2$ . the fluid velocity increases while the angular velocity decreases to  $h(\eta) \approx -0.4$  and then increases to zero when  $\lambda$  increases as depicted in Figure 21 and Figure 22 respectively. Meanwhile, the temperature behavior decreases due to the presence of  $\lambda$ .

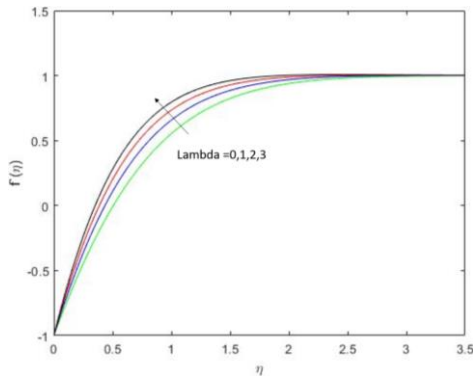


**Fig. 20.** Velocity profile  $f''(\eta)$  for varies of  $\lambda$

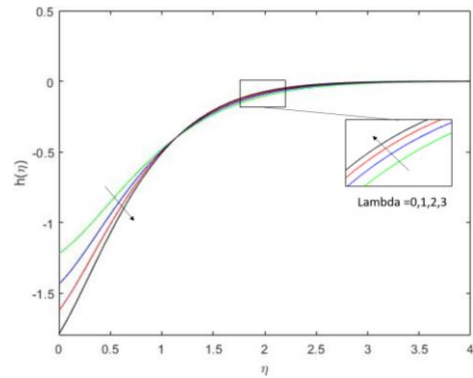


**Fig. 21.** Angular velocity profile  $h'(\eta)$  for varies of  $\lambda$

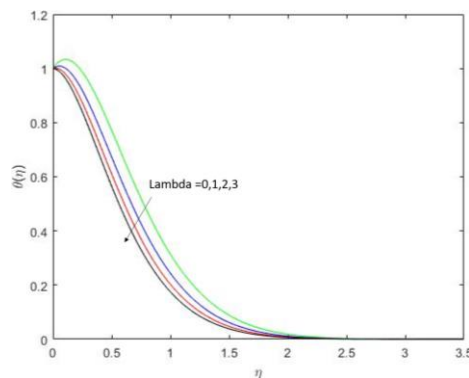


**Fig. 22.** Temperature profile  $\theta(\eta)$  for varies of  $\lambda$

The Figure 23, Figure 24 and Figure 25 illustrate the effects on radiation parameter  $R$  where  $R=0,1,3,5$ . The fluid velocity  $f''(\eta)$  and angular velocity  $h'(\eta)$  increases due to the impact of increasing in  $R$  as shown in the Figure 23 and Figure 24. While the  $\theta(\eta)$  show the two phenomena which are decreases to  $\theta(\eta) \approx 0.6$  and then increases as shown in Figure 25.

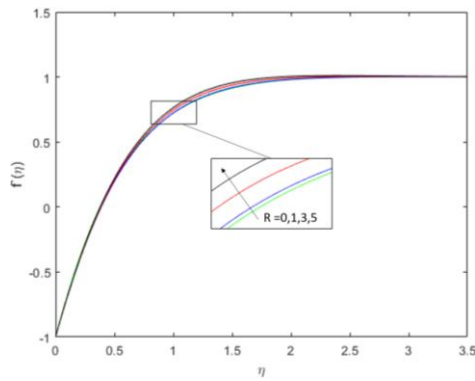


**Fig. 23.** Velocity profile  $f''(\eta)$  for varies of  $R$

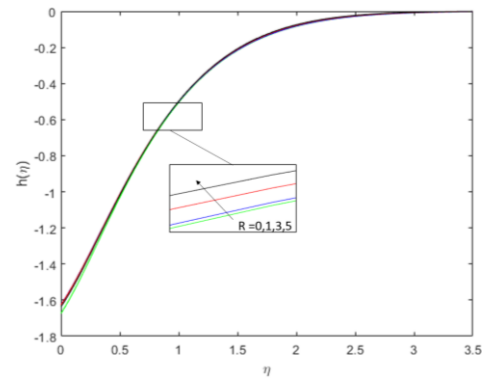


**Fig. 24.** Angular velocity profile  $h'(\eta)$  for varies of  $R$

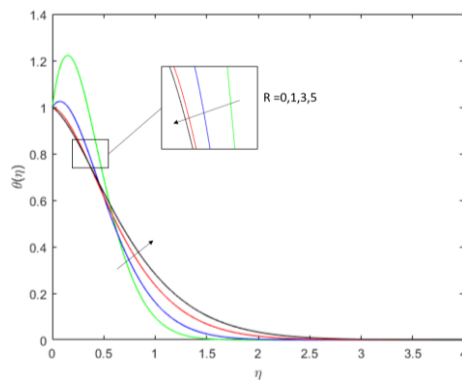


**Fig. 25.** Temperature profile  $\theta(\eta)$  for varies of  $R$

#### 4. Conclusions

The problem of MHD stagnation point flow and heat transfer over an exponentially stretching/shrinking vertical sheet in a micropolar fluid with a buoyancy effect was explored for first solution. The governing PDEs were transformed to ODEs using suitable similarity transformation. The existence of the stretching/shrinking solution was discovered. The collective impact of micropolar, buoyancy force, magnetic field and radiation over an exponentially stretching/shrinking vertical plate are described. This study's findings provide an analysis of flow and heat transfer in a micropolar fluid that will aid other researchers or engineers in selecting appropriate parameters for heat transfer optimization in modern industry. From this present paper, we detect the following:

- a) An increase of micropolar parameter leads to a decrease of the velocity profile and increase the temperature profile, but angular profile on the surface increase at the beginning and then decrease to the boundary layers.
- b) The skin friction for micropolar parameter shows the upper and lower trend at shrink surface and then increase for stretch surface. It means that the movement of the fluid become tough in the beginning. The same trend can be found for the couple stress when an increase of micropolar parameter.
- c) The similar behaviour was observed when magnetic and buoyancy parameters were increased, which increases the velocity and decreases the temperature profiles, respectively. Also, the angular velocity drops at first and subsequently increases for the stretch surface.

- d) As the buoyancy parameter is increased, the skin friction, couple stress, and Nusselt number increase.
- e) The radiation parameter increment displays upper trends for the velocity and angular profiles. The same holds for skin friction and couple stress.

### Acknowledgment

This research was funded by a grant from the Ministry of Higher Education of Malaysia (FRGS/1/2021/STG06/UITM/02/11) and Universiti Teknologi MARA Shah Alam is gratefully acknowledged.

### References

- [1] Lund, Liaquat Ali, Zurni Omar, Ilyas Khan, Dumitru Baleanu, and Kottakkaran Sooppy Nisar. "Convective effect on magnetohydrodynamic (MHD) stagnation point flow of Casson fluid over a vertical exponentially stretching/shrinking surface: Triple solutions." *Symmetry* 12, no. 8 (2020): 1238. <https://doi.org/10.3390/sym12081238>
- [2] Dash, G. C., R. S. Tripathy, M. M. Rashidi, and S. R. Mishra. "Numerical approach to boundary layer stagnation-point flow past a stretching/shrinking sheet." *Journal of Molecular Liquids* 221 (2016): 860-866. <https://doi.org/10.1016/j.molliq.2016.06.072>
- [3] Crane, Lawrence J. "Flow past a stretching plate." *Zeitschrift für angewandte Mathematik und Physik ZAMP* 21, no. 4 (1970): 645-647. <https://doi.org/10.1007/BF01587695>
- [4] Soid, Siti Khuzaimah, Anuar Ishak, and Ioan Pop. "MHD stagnation-point flow over a stretching/shrinking sheet in a micropolar fluid with a slip boundary." *Sains Malaysiana* 47, no. 11 (2018): 2907-2916. <https://doi.org/10.17576/jsm-2018-4711-34>
- [5] Shu, Jian-Jun, and Jenn Shiun Lee. "Fundamental solutions for micropolar fluids." *Journal of Engineering Mathematics* 61, no. 1 (2008): 69-79. <https://doi.org/10.1007/s10665-007-9160-8>
- [6] Nazar, Roslinda, Norsarahaida Amin, Diana Filip, and Ioan Pop. "Stagnation point flow of a micropolar fluid towards a stretching sheet." *International Journal of Non-Linear Mechanics* 39, no. 7 (2004): 1227-1235. <https://doi.org/10.1016/j.ijnonlinmec.2003.08.007>
- [7] Ishak, Anuar, Yian Yian Lok, and Ioan Pop. "Stagnation-point flow over a shrinking sheet in a micropolar fluid." *Chemical Engineering Communications* 197, no. 11 (2010): 1417-1427. <https://doi.org/10.1080/00986441003626169>
- [8] Borrelli, Alessandra, Giulia Giantesio, and Maria Cristina Patria. "Numerical simulations of three-dimensional MHD stagnation-point flow of a micropolar fluid." *Computers & Mathematics with Applications* 66, no. 4 (2013): 472-489. <https://doi.org/10.1016/j.camwa.2013.05.023>
- [9] Attia, Hazem Ali. "Stagnation point flow and heat transfer of a micropolar fluid with uniform suction or blowing." *Journal of the Brazilian Society of Mechanical Sciences and Engineering* 30 (2008): 51-55. <https://doi.org/10.1590/S1678-58782008000100008>
- [10] Mishra, S. R., I. Khan, Q. M. Al-Mdallal, and T. Asifa. "Free convective micropolar fluid flow and heat transfer over a shrinking sheet with heat source." *Case Studies in Thermal Engineering* 11 (2018): 113-119. <https://doi.org/10.1016/j.csite.2018.01.005>
- [11] Nisar, Kottakkaran Sooppy, Aftab Ahmed Faridi, Sohail Ahmad, Nargis Khan, Kashif Ali, Wasim Jamshed, Abdel-Haleem Abdel-Aty, and I. S. Yahia. "Cumulative impact of micropolar fluid and porosity on MHD channel flow: a numerical study." *Coatings* 12, no. 1 (2022): 93. <https://doi.org/10.3390/coatings12010093>
- [12] Abbas, Nadeem, S. Nadeem, and M. N. Khan. "Numerical analysis of unsteady magnetized micropolar fluid flow over a curved surface." *Journal of Thermal Analysis and Calorimetry* 147, no. 11 (2022): 6449-6459. <https://doi.org/10.1007/s10973-021-10913-0>
- [13] Reddy, S. R. R., and P. Bala Anki Reddy. "Thermal radiation effect on unsteady three-dimensional MHD flow of micropolar fluid over a horizontal surface of a parabola of revolution." *Propulsion and Power Research* 11, no. 1 (2022): 129-142. <https://doi.org/10.1016/j.jprr.2022.01.001>
- [14] Qian, Wei-Mao, M. Ijaz Khan, Faisal Shah, Mair Khan, Yu-Ming Chu, Waqar A. Khan, and Mubbashar Nazeer. "Mathematical modeling and MHD flow of micropolar fluid toward an exponential curved surface: heat analysis via ohmic heating and heat source/sink." *Arabian Journal for Science and Engineering* 47, no. 1 (2022): 867-878. <https://doi.org/10.1007/s13369-021-05673-w>

- [15] Goud, B. Shankar, Yanala Dharmendar Reddy, Nawal A. Alshehri, Wasim Jamshed, Rabia Safdar, Mohamed R. Eid, and Mohamed Lamjed Bouazizi. "Numerical Case Study of Chemical Reaction Impact on MHD Micropolar Fluid Flow Past over a Vertical Riga Plate." *Materials* 15, no. 12 (2022): 4060. <https://doi.org/10.3390/ma15124060>
- [16] Lakshmi Devi, G., H. Niranjana, and S. Sivasankaran. "Effects of chemical reactions, radiation, and activation energy on MHD buoyancy induced nano fluidflow past a vertical surface." *Scientia Iranica* 29, no. 1 (2022): 90-100.
- [17] Song, Ying-Qing, Hassan Waqas, Shan Ali Khan, Sami Ullah Khan, M. Ijaz Khan, Yu-Ming Chu, and Sumaira Qayyum. "Nonlinear thermally radiative heat transport for brinkman type micropolar nano-material over an inclined surface with motile microorganisms and exponential heat source." *International Communications in Heat and Mass Transfer* 126 (2021): 105351. <https://doi.org/10.1016/j.icheatmasstransfer.2021.105351>
- [18] Asghar, Adnan, Teh Yuan Ying, and Khairy Zaimi. "Two-Dimensional Magnetized Mixed Convection Hybrid Nanofluid Over a Vertical Exponentially Shrinking Sheet by Thermal Radiation, Joule Heating, Velocity and Thermal Slip Conditions." *Journal of Advanced Research in Fluid Mechanics and Thermal Sciences* 95, no. 2 (2022): 159-179. <https://doi.org/10.37934/arfmts.95.2.159179>
- [19] Jahan, Sultana, M. Ferdows, Md Shamshuddin, and Khairy Zaimi. "Radiative Mixed Convection Flow Over a Moving Needle Saturated with Non-Isothermal Hybrid Nanofluid." *Journal of Advanced Research in Fluid Mechanics and Thermal Sciences* 88, no. 1 (2021): 81-93. <https://doi.org/10.37934/arfmts.88.1.8193>
- [20] Widodo, Basuki, Adhi Surya Nugraha, and Tri Rahayuningsih. "Numerical Solution of Mixed Convection MHD Viscous Fluid Flow on Lower Stagnation Point of a Sliced Magnetic Sphere." *Journal of Advanced Research in Fluid Mechanics and Thermal Sciences* 95, no. 1 (2022): 110-120. <https://doi.org/10.37934/arfmts.95.1.110120>
- [21] Mahdy, A., Taghreed H. Al-Arabi, Ahmed M. Rashad, and Wafaa Saad. "Influence Of Thermal Radiation on Unsteady Mixed Convection Flow of Hybrid Nanofluid Past an Elongated Sheet." *Journal of Advanced Research in Fluid Mechanics and Thermal Sciences* 94, no. 2 (2022): 110-122. <https://doi.org/10.37934/arfmts.94.2.110122>
- [22] Ali, I. R., Ammar I. Alsabery, Norhaliza Abu Bakar, and Rozaini Roslan. "Mixed Convection in a Lid-Driven Horizontal Rectangular Cavity Filled with Hybrid Nanofluid by Finite Volume Method." *Journal of Advanced Research in Fluid Mechanics and Thermal Sciences* 93, no. 1 (2022): 110-122. <https://doi.org/10.37934/arfmts.93.1.110122>
- [23] Yasin, Siti Hanani Mat, Muhammad Khairul Anuar Mohamed, Zulkhibri Ismail, Basuki Widodo, and Mohd Zuki Salleh. "Numerical Investigation of Ferrofluid Flow at Lower Stagnation Point over a Solid Sphere using Keller-Box Method." *Journal of Advanced Research in Fluid Mechanics and Thermal Sciences* 94, no. 2 (2022): 200-214. <https://doi.org/10.37934/arfmts.94.2.200214>
- [24] Mopuri, Obulesu, Charankumar Ganteda, Bhagyashree Mahanta, and Giulio Lorenzini. "MHD heat and mass transfer steady flow of a convective fluid through a porous plate in the presence of multiple parameters." *Journal of Advanced Research in Fluid Mechanics and Thermal Sciences* 89, no. 2 (2022): 56-75. <https://doi.org/10.37934/arfmts.89.2.5675>
- [25] Khan, Ansab Azam, Khairy Zaimi, Suliadi Firdaus Sufahani, and Mohammad Ferdows. "MHD flow and heat transfer of double stratified micropolar fluid over a vertical permeable shrinking/stretching sheet with chemical reaction and heat source." *Journal of Advanced Research in Applied Sciences and Engineering Technology* 21, no. 1 (2020): 1-14. <https://doi.org/10.37934/araset.21.1.114>
- [26] Raju, Chakravarthula SK, and Naramgari Sandeep. "Dual solutions for unsteady heat and mass transfer in bio-convection flow towards a rotating cone/plate in a rotating fluid." In *International Journal of Engineering Research in Africa*, vol. 20, pp. 161-176. Trans Tech Publications Ltd, 2016. <https://doi.org/10.4028/www.scientific.net/JERA.20.161>
- [27] Zohra, Fatema T., Mohammed J. Uddin, and Ahamd I. M. Ismail. "Magnetohydrodynamic bio-nanoconvective Naiver slip flow of micropolar fluid in a stretchable horizontal channel." *Heat Transfer-Asian Research* 48, no. 8 (2019): 3636-3656. <https://doi.org/10.1002/htj.21560>
- [28] Soid, Siti Khuzaimah, Anuar Ishak, and Ioan Pop. "Unsteady MHD flow and heat transfer over a shrinking sheet with ohmic heating." *Chinese Journal of Physics* 55, no. 4 (2017): 1626-1636. <https://doi.org/10.1016/j.cjph.2017.05.001>
- [29] Lund, Liaquat Ali, Zurni Omar, Ilyas Khan, Dumitru Baleanu, and Kottakkaran Sooppy Nisar. "Dual similarity solutions of MHD stagnation point flow of Casson fluid with effect of thermal radiation and viscous dissipation: stability analysis." *Scientific Reports* 10, no. 1 (2020): 1-13. <https://doi.org/10.1038/s41598-020-72266-2>
- [30] Waini, Iskandar, Anuar Ishak, and Ioan Pop. "Hybrid nanofluid flow towards a stagnation point on an exponentially stretching/shrinking vertical sheet with buoyancy effects." *International Journal of Numerical Methods for Heat & Fluid Flow* 31, no. 1 (2020): 216-235. <https://doi.org/10.1108/HFF-02-2020-0086>
- [31] Uddin, Md Sharif, Krishnendu Bhattacharyya, and Sharidan Shafie. "Micropolar fluid flow and heat transfer over an exponentially permeable shrinking sheet." *Propulsion and Power Research* 5, no. 4 (2016): 310-317. <https://doi.org/10.1016/j.jprr.2016.11.005>
- [32] Siddiq, Sadia, Naheed Begum, Md Anwar Hossain, Muhammad Nasir Abrar, Rama Subba Reddy Gorla, and Qasem Al-Mdallal. "Effect of thermal radiation on conjugate natural convection flow of a micropolar fluid along a vertical

- surface." *Computers & Mathematics with Applications* 83 (2021): 74-83. <https://doi.org/10.1016/j.camwa.2020.01.011>
- [33] Rehman, Fiaz Ur, Sohail Nadeem, Hafeez Ur Rehman, and Rizwan Ul Haq. "Thermophysical analysis for three-dimensional MHD stagnation-point flow of nano-material influenced by an exponential stretching surface." *Results in Physics* 8 (2018): 316-323. <https://doi.org/10.1016/j.rinp.2017.12.026>
- [34] Reddy, G. Janardhana, Bhaskerreddy Kethireddy, and H. P. Rani. "Bejan's heat flow visualization for unsteady micropolar fluid past a vertical slender hollow cylinder with large Grashof number." *International Journal of Applied and Computational Mathematics* 4, no. 1 (2018): 1-25. <https://doi.org/10.1007/s40819-017-0468-4>
- [35] Mutegi, R. A., John Achola Okello, and M. Kimathi. "Analysis of Effect of Inclined Magnetic Field on MHD Boundary Layer Flow over a Porous Exponentially Stretching Sheet Subject to Thermal Radiation." *Asian Research Journal of Mathematics* 17, no. 9 (2021): 20-33. <https://doi.org/10.9734/arjom/2021/v17i930328>
- [36] Abdul Halim, Nadhirah, and Noor Fadiya Mohd Noor. "Mixed convection flow of Powell-Eyring nanofluid near a stagnation point along a vertical stretching sheet." *Mathematics* 9, no. 4 (2021): 364. <https://doi.org/10.3390/math9040364>